Microscale digital twinning of rubble stone masonry walls using robotic assembly

Qianqing Wang[1], Jingwen Wang[2], Stefana Parascho[2], Katrin Beyer[1]

[1]Earthquake Engineering and Structural Dynamics Laboratory (EESD), EPFL, 1015 Lausanne, Switzerland
[2]Lab for Creative Computation (CRCL), EPFL, 1015 Lausanne, Switzerland

qianqing.wang@epfl.ch, jingwen.wang@epfl.ch, stefana.parascho@epfl.ch, katrin.beyer@epfl.ch

Abstract -

This paper presents a novel method for generating microscale digital twins of rubble stone masonry walls using a robotic construction pipeline. The pipeline integrates stone stock digitalization, stone layout planning, robotic stone assembly, and a dynamic digital twinning process. To validate the approach, a $0.7 \times 0.7 \times 0.4$ m^3 wall was physically constructed in the lab alongside its digital twin, which provided a precise representation of the wall's microstructures. The results show that the proposed pipeline achieved accurate stone assembly with an averaged ±1.2 cm tolerance, producing walls comparable to traditional masonry in terms of compressive strength.

Keywords -

Stone masonry wall; Digital twin; Robotic assembly; Natural stone; Simple compression test

1 Introduction

The construction industry urgently requires innovative solutions to reduce its environmental impact. Utilizing locally available natural materials, such as stone, offers a sustainable path by minimizing energy inputs and carbon emissions associated with material production and transportation [1, 2]. However, traditional stone construction poses challenges for the structural analysis. The irregular shapes of stone units and their placement based on local masonry practices create a highly variable microstructure, which directly impacts the structural behavior of stone masonry building [3]. Current practice for the structural analysis of rubble stone masonry buildings rely on fixed-length classifications based on typologies, which are subjective and introduce ambiguity in the analysis [3].

With advancements in digital technologies, it is now possible to create a digital twin, a 3D model of a physical asset. In masonry structures, digital twinning at the building level—where entire structures are scanned, digitized, and used for numerical analysis—has been explored by several works [4, 5, 6]. However, digital twinning at the stone-level, capturing the as-built microstructure [3], remains rare. This lack of detailed digital twins for stone masonry microstructures poses a significant bottleneck in the development of micro-scale numerical methods for analyzing rubble stone masonry structures [3].

This paper introduces an end-to-end pipeline for generating the microscale digital twin of stone masonry structures, utilizing a novel construction method that eliminates the need for masons. It starts from digitalizing the irregular shape of stones using photogrammetry. The 3D geometry of stones is used by a planning algorithm to determine the positions and orientation of stones. The execution of the plan, i.e., placing stones from the initial position to the final position in the wall, is carried out by a robotic system composed of a vacuum gripper, an on-site scanning system, and a robotic arm. A digital twining pipeline is carried out at the same time as the physical construction, recording the as-built position of stones, which feedbacks the planning algorithm to achieve a more precise and accurate construction.

2 Method

This section presents the main components of the proposed pipeline for the digital construction of mortar-joint stone masonry walls. Section 2.1 presents the methods and results of using photogrammetry to build the digital stone stock. The construction process is explained in Section 2.2, which includes the optimization of the stone layout, the physical construction, and the creation of the digital twin.

2.1 Digitization of initial stone stock

. We scanned 150 stones that were recycled from the demolition waste of stone masonry walls built by masons. The stones were scanned by capturing 100 photographs of one side, then flipping them over and taking an additional 100 photos of the opposite side. The photos were taken with a robotic arm that rotates around the object and takes photos at every 18-degree interval. The 200 photos were used for 3D model reconstruction with the software Agisoft Metashape [7]. A scaled bar is also visible in all photos with specific markers supported by Agisoft Metashape [7]. Figure 1 shows the distribution of stone shapes and stone sizes in the initial stock. Stones that are not placed in the constructed wall are indicated by circles in Figure 1. Stone flatness is measured by the ratio of the shortest

dimension to the intermediate dimension, and elongation is measured by the ratio of the intermediate dimension to the longest dimension, with dimension sizes determined through the principal component analysis [8].

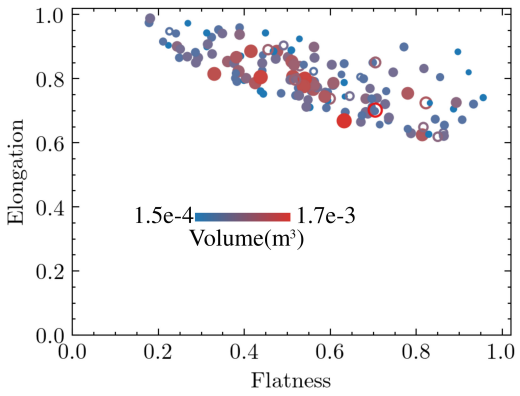

Figure 1. Elongation, flatness, and volume of stones in the initial stock. Stones not used in the final wall are shown by unfilled circles, while others are shown by filled points.

2.2 Microscale digital twinning by segment-wise construction

We propose a segment-wise construction and digital twinning process, where one segment corresponds to elevating the wall with a certain height according to the construction progress during the day. Figure 2 presents the steps for constructing one segment. Before the physical construction of a segment, the layout planning algorithm determines the stone layout for the current segment considering the current landscape, which is composed of the digital twin of previous segments and the boundary condition. The planning of stone layout is followed by the physical construction, where a robotic arm places stones to their planned positions. The robotic assembly of stones is paused every time a new layer of stones was placed on top of an existing one. During the pause, the physical wall is scanned by taking photos around it to capture the as-built positions of stones. We generate the digital twin of the segment based on the scanned layers, which serves as the input for planning and constructing the subsequent segments. Mortar layers are applied manually between layers. We will present in the following sections the details regarding the layout planning, robotic construction, and digital twinning.

2.2.1 Stone layout planning

To generate the stone layout in each segment, the planning algorithm developed in our previous work [9, 10] is used. We adapt the algorithm for segment-wise planning by including two additional functions. One is to apply a mask on top of every segment to avoid stones being placed beyond the segment height. It constrains the algorithm to find feasible positions only below the upper bound. The mask is implemented as assigning the value 1 to voxels above the current segment in the landscape occupancy tensor $L_{\text{occupancy}}$. The other improvement is to use the digital twin of stones from previous segments instead of using their planned positions to account for deviations of stone positions that can arise during the physical construction. As an example, Figure 3 shows the landscape for constructing one segment, composed of five parts: the as-built position of already placed stones from previous segments (in green), the planning positions of stones of the current segment (in blue), the boundaries of the wall (in grey), and the mask for limiting the upper bound (in black).

2.2.2 Robotic stone assembly

We choose a vacuum gripper instead of the conventional two-finger gripper due to its flexibility in handling objects with varying lengths and widths. After analyzing the shape of the stone, considering its curvature, center of gravity, suction area, and avoidance of collisions with stones placed previously, we determined the optimal picking planes for the stones. A team member manually attaches the stone to the gripper at the calculated position, after which we re-scan the stone to precisely locate its position and orientation relative to the robot end-effector. This data enables accurate calculation of the robot's placement trajectory.

2.2.3 Digital twinning

After placing each layer of stones, we scan the half-built wall with photogrammetry and reconstruct the 3D model with Agisoft Metashape [7]. The mesh is then transformed and rescaled according to the positions of markers in the robot frame, measured at the beginning of the construction. We register the stone mesh (a complete stone mesh) to the landscape mesh (where stones can be observed partially) using ICP [11], transforming the stone from the planning position to the as-built position, as shown in Figure 4.

3 Results

We applied the proposed digital construction pipeline to build a stone masonry wall of size $0.7 \times 0.7 \times 0.4$ m^3. The dimensions were chosen to match the size of mason-built walls of a similar typology, as in [3], ensuring a fair comparison of construction results. Figure 5 shows a photo and the 3D surface mesh of the final wall, as well

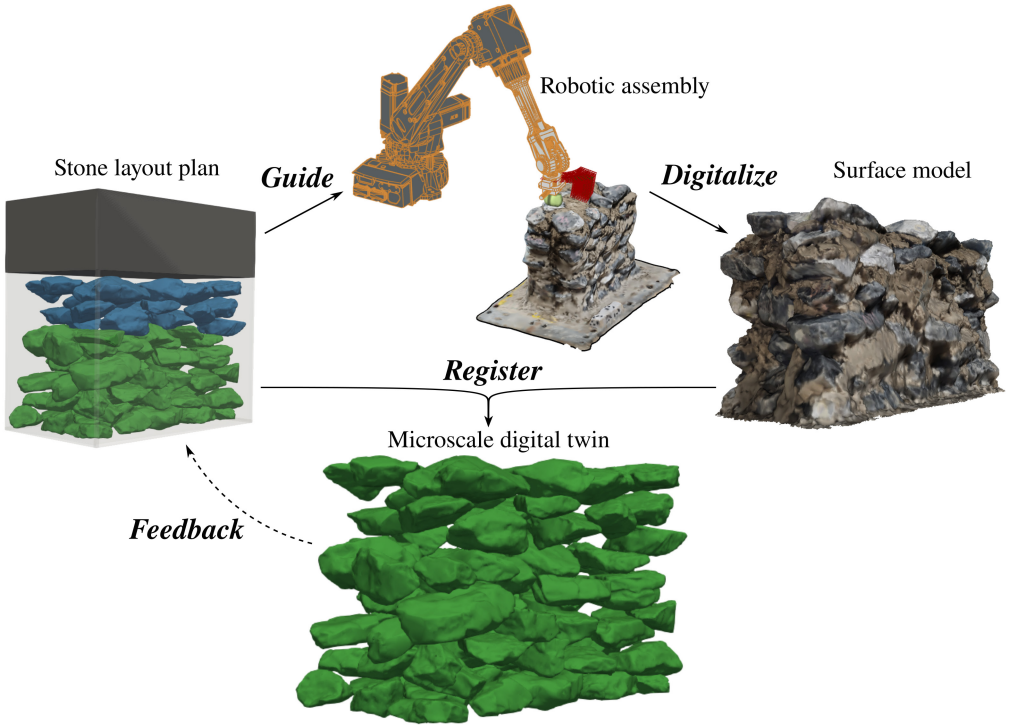

Figure 2. Microscale digital twinning process: starting with the generation of the stone layout plan, followed by robotic assembly guided by the plan, digitalization of the wall surface, and finally, registering the planned stones to the digitized wall to create the microscale digital twin of the as-built stone layout.

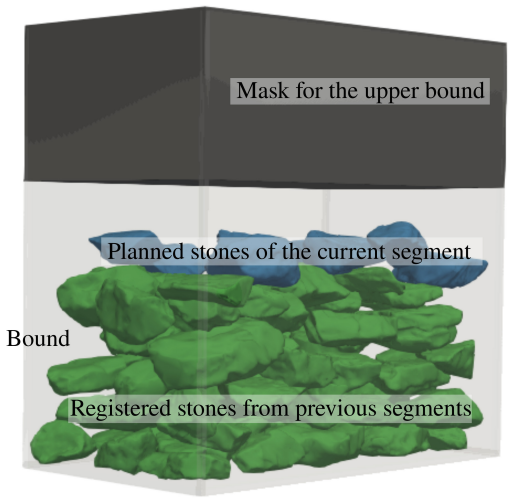

Figure 3. Landscape for planning one segment.

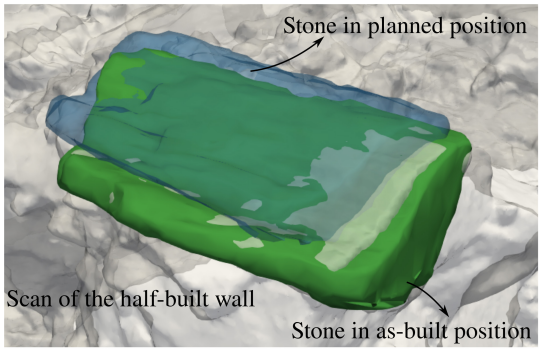

Figure 4. Transforming stones from planned position to as-built position by registering the stone mesh to the landscape mesh.

as its microscale digital twin composed of stone meshes in their as-built positions.

3.1 Simple compression test of the constructed wall

In masonry construction, walls primarily support compressive forces from the weight of the structure above. In this case, compressive strength is a crucial index that directly reflects their load-bearing capacity and resistance to failure under vertical loads. To obtain the compressive strength of the constructed wall, a simple compression test with no confinements at the top and bottom of the specimen was conducted according to the described procedures in EN1015-Part 1 [12]. In the compression tests, three loading/unloading cycles were applied before the peak force. The Young's modulus was derived by fitting a line to each of the three stress–strain cycles and taking the average value of the three slopes as presented in [13]. We obtained a compressive strength of 0.74 MPa, and a Young's modulus of 263 MPa. The strength is within the range reported in [14], between 0.43 MPa and 0.82 MPa.

3.2 Precision in stone assembly

To quantify the precision of the stone assembly process, we made use of the microscale digital twin obtained as the end of the construction, measuring the distances between the as-built positions of stones and their planned positions. We observed an averaged distance between stone centers of 0.012 m and a root mean square error of 0.014 m. The difference between the as-built geometry and planned geometry can be attributed to the following reasons:

1. When the robot reaches the force limit, it will release the stone before it arrives to its planned position.
2. The planned position of the stone is not necessarily a stable position. The stone can move under gravity after robot release it.
3. There are systematic errors in the digital twinning process, including the downsampling of stone meshes for robotic planning and layout planning, the registration of stone mesh to gripping position, the reconstruction of landscape mesh, and the registration of stone mesh to landscape mesh.

Situation 1 consistently happened when placing the first layer of stones. This is because the planning assumes the foundation to be perfectly flat, while the small bumps on the foundation stop the stone placement earlier. The error didn't propagate to the next segment of stones as the planning algorithm considered an updated landscape. For the following layers, stones were mostly placed below their planned position due to the effect of gravity, especially stones on the corners.

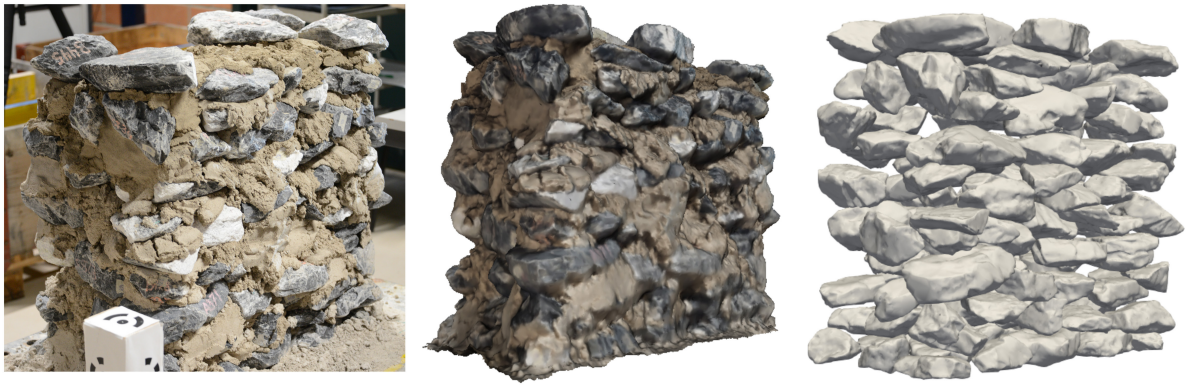

(a) (b) (c)

Figure 5. The constructed wall. (a) Photo of the constructed wall. (b) 3D surface model of the final wall. (c) Stones in the final wall on their as-built positions.

4 Conclusions

The traditional construction of masonry structures using natural stones often faces challenges in structural analysis due to the uncertainty and variability of the microstructure. This study introduces a pioneering pipeline for generating the microscale digital twin of stone masonry walls, which replicates the microstructure of physical walls. The pipeline makes use of the recent advance in stone layout optimization [9], to instruct a robotic system for stone assembly. The microscale digital twin is created at the same time of the physical construction, providing dynamic feedback for the construction process.

A three-leaf masonry wall was built as a case study to show the feasibility of the proposed method. Results show that the constructed wall achieved compressive strength of 0.74 MPa, and the digital twinning process had an averaged distance error of 0.012 m. While this work demonstrates the feasibility of digital masonry construction, further advancements in the digitalization of mortar are essential to fully realize the pipeline's potential.

References

[1] J.C Morel, A Mesbah, M Oggero, and P Walker. Building houses with local materials: means to drastically reduce the environmental impact of construction. *Building and Environment*, 36 (10):1119–1126, dec 2001. doi:10.1016/s0360-1323(00)00054-8. URL https://doi.org/10.1016%2Fs0360-1323%2800%2900054-8.

[2] R. Přikryl, Á. Török, M. Theodoridou, M. Gomez-Heras, and K. Miskovsky. Geomaterials in construction and their sustainability: understanding their role in modern society. *Geological Society, London, Special Publications*, 416(1):1–22, January 2016. ISSN 2041-4927. doi:10.1144/sp416.21. URL http://dx.doi.org/10.1144/sp416.21.

[3] Savvas Saloustros, Andrea Settimi, Andrea Cabriada Ascencio, Julien Gamerro, Yves Weinand, and Katrin Beyer. Geometrical digital twins of the as-built microstructure of three-leaf stone masonry walls with laser scanning. *Scientific Data*, 10(1), August 2023. ISSN 2052-4463. doi:10.1038/s41597-023-02417-3. URL http://dx.doi.org/10.1038/s41597-023-02417-3.

[4] Emerson Cuadros-Rojas, Savvas Saloustros, Nicola Tarque, and Luca Pelà. Photogrammetry-aided numerical seismic assessment of historical structures composed of adobe, stone and brick masonry. application to the san juan bautista church built on the inca temple of huaytará, peru. *Engineering Failure Analysis*, 158:107984, April 2024. ISSN 1350-6307. doi:10.1016/j.engfailanal.2024.107984. URL http://dx.doi.org/10.1016/j.engfailanal.2024.107984.

[5] Bryan German Pantoja-Rosero, Radhakrishna Achanta, and Katrin Beyer. Automated image-based generation of finite element models for masonry buildings. *Bulletin of Earthquake Engineering*, 22(7):3441–3469, June 2023. ISSN 1573-1456. doi:10.1007/s10518-023-01726-7. URL http://dx.doi.org/10.1007/s10518-023-01726-7.

[6] A.M. D'Altri, S. de Miranda, G. Castellazzi, and B. Glisic. Numerical modelling-based damage diagnostics in cultural heritage structures. *Jour-*

nal of Cultural Heritage, 61:1–12, May 2023. ISSN 1296-2074. doi:10.1016/j.culher.2023.02.004. URL http://dx.doi.org/10.1016/j.culher.2023.02.004.

[7] AgiSoft. Photoscan professional, 2016. Software.

[8] Deheng Wei, Jianfeng Wang, and Budi Zhao. A simple method for particle shape generation with spherical harmonics. *Powder Technology*, 330:284–291, May 2018. ISSN 0032-5910. doi:10.1016/j.powtec.2018.02.006. URL http://dx.doi.org/10.1016/j.powtec.2018.02.006.

[9] Qianqing Wang, Ketson R.M. dos Santos, and Katrin Beyer. Geometric planning for masonry wall construction with natural stones using discrete convolution. *Engineering Structures*, 329:119695, April 2025. ISSN 0141-0296. doi:10.1016/j.engstruct.2025.119695. URL http://dx.doi.org/10.1016/j.engstruct.2025.119695.

[10] Qianqing Wang, Bryan German Pantoja-Rosero, Ketson R.M. dos Santos, and Katrin Beyer. An image convolution-based method for the irregular stone packing problem in masonry wall construction. *European Journal of Operational Research*, 316(2):733–753, July 2024. ISSN 0377-2217. doi:10.1016/j.ejor.2024.01.037. URL http://dx.doi.org/10.1016/j.ejor.2024.01.037.

[11] Paul J. Besl and Neil D. McKay. A method for registration of 3-d shapes. *IEEE Transactions on Pattern Analysis and Machine Intelligence*, 14(2):239–256, 1992. doi:10.1109/34.121791.

[12] BS EN. 1052-1: Methods of test for masonry, part 1: Determination of compressive strength. *British Standards Institution, London, UK*, 1999.

[13] Amir Rezaie, Michele Godio, and Katrin Beyer. Experimental investigation of strength, stiffness and drift capacity of rubble stone masonry walls. *Construction and Building Materials*, 251:118972, August 2020. ISSN 0950-0618. doi:10.1016/j.conbuildmat.2020.118972. URL http://dx.doi.org/10.1016/j.conbuildmat.2020.118972.

[14] Savvas Saloustros and Katrin Beyer. *Experimental Investigation on Size-Effect of Rubble Stone Masonry Walls Under In-Plane Horizontal Loading: Overview and Preliminary Results*, page 463–471. Springer Nature Switzerland, September 2023. ISBN 9783031396038. doi:10.1007/978-3-031-39603-8_38. URL http://dx.doi.org/10.1007/978-3-031-39603-8_38.